Mixed valence and metamagnetism in a metal flux grown compound $Eu_2Pt_3Si_5$

Sumanta Sarkar [a], Udumula Subbarao [a], Boby Joseph [b], Sebastian C. Peter [a,*]

[a] New Chemistry Unit, Jawaharlal Nehru Centre for Advanced Scientific Research, Jakkur, Bangalore 560064, India
[b] Elettra–Sincrotrone Trieste SCpA, SS14 Km 163.5, 34149 Basovizza, Trieste, Italy

ABSTRACT

A new compound $Eu_2Pt_3Si_5$ with plate shaped morphology has been grown from excess In flux. The compound crystallizes in the orthorhombic $U_2Co_3Si_5$ structure type, Ibam space group and the lattice parameters are $a = 10.007(2)$ Å, $b = 11.666(2)$ Å and $c = 6.0011(12)$ Å. The crystal structure of this compound can be conceived as inter-twinned chains of $[Pt_2Si_2]$ and $[PtSi_3]$ tetrahedra connected along [100] direction to give rise to a complex three dimensional $[Pt_3Si_5]$ network. Temperature dependent magnetic susceptibility data suggests that $Eu_2Pt_3Si_5$ undergoes a strong antiferromagnetic ordering ($T_N = 19$ K) followed by a weak ferromagnetic transition ($T_C = 5.5$ K). The effective magnetic moment/Eu obtained from susceptibility data is 6.78 μ_B accounts mixed valent Eu with almost 85% divalent Eu, which is supported by X-ray absorption near edge spectroscopy. The compound undergoes a metamagnetic transition under applied magnetic field through a probable spin flop mechanism.

© 2015 Elsevier Inc. All rights reserved.

1. Introduction

The physical properties of rare earth based materials, particularly intermetallic compounds are mostly governed by the f electrons which largely contribute to the valence state of these materials. Among those, compounds with heavier transition metals i.e. 4d and 5d series of transition metals are even more fascinating as the hybridization of 4f and itinerant conduction electrons primarily from the d orbitals of the transition metals gives rise to anomalous properties [1–5]. Some of these anomalous properties include Kondo-type behavior in concentrated systems, high magnetic ordering temperature and heavy fermion behavior. Valence-fluctuating behavior is a notable property among Eu, Yb, and Ce based compounds [6–8]. Ce based compounds have undoubtedly dominated over others because of mainly three reasons; first, the compounds containing Ce are relatively more stable in air than the corresponding Eu and Yb analogs and hence it is easier to study these compounds, second, only one 4f electron in Ce makes it a lot easier to study and explain the structural and physical properties [9] and third, Ce based compounds can be synthesized by the conventional methods easily compared to Eu and Yb. However, recently, we have succeeded in the synthesis of several Eu and Yb based compounds using a metal flux technique [1,10–28].

The compounds with the general formula $RE_2T_3X_5$ (RE = Rare earth elements, T = Transition metals, X = p-block elements) have

been studied in the past few decades owing to the broad diversity in their structure and physical properties. A few interesting examples are: antiferromagnetic Kondo lattice in $Ce_2Pt_3Si_5$ [29,30], CEF-split singlet state in $Pr_2Pt_3Si_5$ [31], low temperature superconductivity in $Er_2Fe_3Si_5$ [32], $Tm_2Fe_3Si_5$ [33], $Lu_2Fe_3Si_5$ [34], $La_2Ir_3Ge_5$ [35] and $Y_2Ir_3Ge_5$ [35], multigap superconductivity in $Pr_2Pt_3Ge_5$ [36] and valence fluctuation in $Ce_2Co_3Ge_5$ and $Ce_2Ni_3Ge_5$ [37,38].

The compounds with general formula $RE_2T_3X_5$ crystallize in different orthorhombic crystal structure types: $U_2Co_3Si_5$ type (Ibam) [39], $Yb_2Ir_3Ge_5$ type (Pmmn) [40], $Yb_2Pt_3Sn_5$ type (Pnma) [41], $Ln_2Au_3In_5$ type ($Pmn2_1$) [42] and $Yb_2Au_3In_5$ type ($Cmc2_1$) [18]. Some of the compounds are also known to crystallize in tetragonal $Sc_2Fe_3Si_5$ [43] or $U_2Mn_3Si_5$ [44] type structures and monoclinic $Lu_2Co_3Si_5$ structure type (C2/c) [45]. The key synthetic strategies used so far for studying the physical properties of these compounds are arc melting and induction furnace methods. However, there are handful reports on single crystals growth by metal flux technique, e.g. single crystals of $Ce_2Rh_3Ge_5$ were synthesized using Bi flux [46], $RE_2Ni_{3+x}Si_{5+x}$ (RE = Sm, Gd and Tb) were synthesized by Ga flux [47], $Yb_2Au_3In_5$ was synthesized using In as active flux [18] and Sn flux was used to obtain $Ce_2Ni_3Si_5$ single crystals from pre-synthesized melt [38]. To the best of our knowledge only following lanthanides are reported in the series $RE_2Pt_3Si_5$ (RE = La, Ce, Pr, Sm, Gd, Yb) [29–31,48–50].

So far there are three compounds reported in the Eu–Pt–Si series, EuPtSi crystallizing in cubic $P2_13$ space group [51], two different tetragonal structures were reported for $EuPt_2Si_2$ (I4/mmm and P4/nmm) [52,53] and $EuPt_{1.075}Si_{1.925}$ crystallizes in orthorhombic Cmcm

* Corresponding author. Tel.: +91 080 22082998; fax: +91 080 22082627.
E-mail address: sebastiancp@jncasr.ac.in (S.C. Peter).

space group [54]. Here we report a new compound in this series, $Eu_2Pt_3Si_5$ synthesized using indium as an inactive metal flux. The compound was characterized by single crystal the X-ray diffraction and SEM–EDAX techniques. The temperature dependent magnetic susceptibility study revealed that the compound is a valence fluctuating system, where as the field dependent magnetization studies hinted toward a metamagnetic transition at relatively higher field. The mixed valent nature of Eu was later confirmed by X-ray Absorption Near Edge Spectroscopy (XANES). Work on other compounds in this series is in progress and their discussion is beyond the scope of this current work.

2. Experimental

2.1. Synthesis

Europium (ingots, 99.99%, ESPI metals), platinum (wire 0.25 mm diameter, 99.9%, Alfa Aesar), silicon (shots, 99.999%, Alfa Aesar) and indium (tear drops, 99.99%, Alfa Aesar) were used as purchased without any further purification.

3 mmol of europium, 2 mmol of platinum, 6 mmol of silicon and 30 mmol of indium were taken in a 4 cm alumina crucible under an inert (argon) atmosphere inside a glove box (H_2O, O_2 levels < 0.1 ppm). The purpose of excess indium was to act as a metal flux. The crucible was placed in a 13 mm quartz tube and was flame-sealed under vacuum of 10^{-4} Torr, to prevent oxidation during heating. The tube was then placed in a vertical tube furnace and heated to 1273 K in 10 h, kept at that temperature for 5 h. The temperature was then lowered down to 1123 K in 2 h and annealed at this temperature for 72 h. Finally, the system was allowed to cool slowly to room temperature in 48 h. The reaction products were isolated from the excess In flux by heating at 623 K and subsequent centrifugation through a coarse frit. The remaining flux was removed by immersion in glacial acetic acid for 1 h. The final crystalline products were rinsed with water and dried with acetone in a vacuum oven at 350 K for 12 h. The compound was grown as shiny thin plate shaped crystals with broad distribution of size. The crystals were not affected by air and moisture and no decomposition was observed even after several months. Single crystals were carefully selected for the elemental analysis, structure characterization and the magnetic measurements. Although our attempts to synthesize the bulk compound by high frequency induction heating were not successful, direct heating of the constituent elements with 2:3:5 M ratio in an evacuated quartz tube at 10^{-4} Torr pressure to 1273 K in 10 h followed annealing for 48 h at the same temperature and cooling to 303 K over 48 h yielded the desired phase ($Eu_2Pt_3Si_5$) with minute quantity of PtSi as the major impurity phase detected by powder the X-ray diffraction technique (Fig. S1).

2.2. Elemental analysis

Quantitative microanalysis on $Eu_2Pt_3Si_5$ was performed with a FEI NOVA NANOSEM 600 instrument equipped with an EDAX® instrument. Data were acquired with an accelerating voltage of 20 kV and a 100 s accumulation time. A typical metallic plate shaped single crystal of $Eu_2Pt_3Si_5$ obtained from the flux method is shown in Fig. S2. The EDAX analysis was performed using a P/B-ZAF standardless method (where, $Z=$ atomic no. correction factor, $A=$ absorption correction factor, $F=$ fluorescence factor, P/B$=$ peak to background model) on visibly clean surfaces of the crystals. The microanalysis on different spots on the crystal gave an average molar composition in good agreement with the composition obtained from the single crystal XRD refinement.

2.3. Single crystal X-ray diffraction

A carefully selected single crystal of $Eu_2Pt_3Si_5$ was mounted on a thin glass fiber. X-ray single crystal structural data for $Eu_2Pt_3Si_5$ were collected at room temperature on a Bruker Smart Apex 2 CCD diffractometer equipped with a normal focus, 2.4 kW sealed tube X-ray source with graphite monochromatic Mo-$K\alpha$ radiation ($\lambda = 0.71073$ Å) operating at 50 kV and 30 mA, with the ω scan mode using a full sphere of 60 frames acquired up to 73.28° in 2θ. The individual frames were measured with steps of 0.50° and an exposure time of 20 s per frame. A crystal of suitable size ($0.15 \times 0.08 \times 0.04$ mm^3) was cut from a plate-shaped crystal and mounted on a thin glass (~ 0.1 mm) fiber with commercially available super glue. The program SAINT [55] was used for integration of diffraction profiles along with the SADABS package suite [56] to apply numerical absorption corrections.

2.4. Powder X-ray diffraction

The phase purity of the sample synthesized by direct heating was determined by analyzing X-ray diffraction data collected on the PANalytical Empyrean diffractometer in alpha-1 geometry equipped with PIXcel^{3D} detector using monochromatized Cu $K\alpha$1 radiation ($\lambda = 1.5406$ Å). in the angular range $10° \leq 2\theta \leq 90°$ with the step size 0.02° and scan rate of 0.5 s/step. The experimental patterns were compared to the pattern simulated from the single crystal structure refinement. The comparison of the powder patterns with the simulated pattern obtained from the single crystal data are shown in Fig. S1.

2.5. Structure refinement

The preliminary data collection on $Eu_2Pt_3Si_5$ at shorter exposure time (10 s, 20 s) did not yield any convincing refinement due to poor intensity of the data but hinted towards an I-centered orthorhombic crystal system and mmm Laue class. Hence, the exposure time was further increased to 30 s. In this case the refinement converged well and the residual parameters became well behaved. The absorption coefficient of the compound was very high due to the presence of Pt and hence absorption correction was done using both multiscan and numerical methods, the former produced better results. The lattice parameters were $a = 10.007(2)$ Å, $b = 11.666(2)$ Å, $c = 6.0011(12)$ Å, respectively were compatible with the $U_2Co_3Si_5$ structure type. EDAX data also hinted a rough composition (atomic%) of 2:3:5 for Eu, Pt and Si, respectively. Therefore, the atomic coordinates of $U_2Co_3Si_5$ were taken as a model and the structures were refined using SHELXL-97 (full-matrix least-squares on F^2) [57] with anisotropic atomic displacement parameters for all atoms. The occupancy parameters were refined in a separate series of least-squares cycles in order to check the correct composition. Finally, the resulting atomic displacement parameters of all positions became well-behaved and the final residual electron densities were reasonably acceptable (2.24 and 3.25e$^-$ A^{-3} respectively). The final compositions of the compound obtained from single crystal XRD data corroborate well with EDAX data. At this point, it is worthwhile to mention that we repeated the entire structure refinement process with the incorporation of indium as a fourth atom which did not improve the refinement to any better extent with residual (R1) and electron density maps values: 2.65% and $\pm 3e^-$ A^{-3}. The EDAX data however did not show any trace of indium in the system and hence establishes the fact that indium acts as an inactive metal flux as already discussed in earlier section. The data collection and refinement parameters $Eu_2Pt_3Si_5$ are summarized in Table 1. The atomic coordinates and equivalent atomic displacement parameters, important bond lengths and anisotropic atomic displacement parameters are listed in Tables 2 and 3 and S1, respectively. Further details on the crystal structure investigation may be obtained from the Fachinformationszentrum Karlsruhe, 76344 Eggenstein-Leopoldshafen, Germany (fax: $+49$–7247-808-666; email; CrysDATA@fiz-karlsruhe.de), on quoting the depository number CSD-428478.

Table 1
Crystal data and structure refinement for $Eu_2Pt_3Si_5$ at 293(2) K.

Empirical formula	$Eu_2Pt_3Si_5$
Formula weight	1029.64
Temperature	293(2) K
Wavelength	0.71073 Å
Crystal system	Orthorhombic
Space group	$Ibam$
Unit cell dimensions	$a = 10.007(2)$ Å,
	$b = 11.666(2)$ Å,
	$c = 6.0011(12)$ Å
Volume	700.6(2) Å^3
Z	4
Density (calculated)	9.762 g/cm^3
Absorption coefficient	78.077 mm^{-1}
$F(000)$	1720
Crystal size	$0.10 \times 0.08 \times 0.04$ mm^3
θ range for data collection	2.68–28.00°
Index ranges	$-13 \leq h \leq 13$, $-15 \leq k \leq 15$, $-7 \leq l \leq 6$
Reflections collected	4027
Independent reflections	466 [$R_{int} = 0.0443$]
Completeness to $\theta = 28.00°$	99.9%
Refinement method	Full-matrix least-squares on F^2
Data/restraints/parameters	466/0/32
Goodness-of-fit	1.475
Final R indices [$> 2\sigma(I)$]	$R_{obs} = 0.0249$, $wR_{obs} = 0.0547$
R indices [all data]	$R_{all} = 0.0270$, $wR_{all} = 0.0840$
Extinction coefficient	0.00048(8)
Largest diff. peak and hole	2.235 and -3.253e Å^{-3}

$R = \Sigma ||F_o| - |F_c|| / \Sigma |F_o|$, $wR = \{\Sigma [w(|F_o|^2 - |F_c|^2)^2] / \Sigma [w(|F_o|^4)]\}^{1/2}$ and calc $w = 1/[\sigma^2(F_o^2) + (0.0603P)^2 + 9.8820P]$ where $P = (F_o^2 + 2F_c^2)/3$.

Table 2
Atomic coordinates ($\times 10^4$) and equivalent isotropic displacement parameters ($Å^2 \times 10^3$) for $Eu_2Pt_3Si_5$ at 293(2) K with estimated standard deviations in parentheses.

Label	x	y	z	Occupancy	U_{eq}[a]
Eu	2656(1)	3708(1)	0	1	7(1)
Pt(1)	5000	0	2500	1	10(1)
Pt(2)	1121(1)	1355(1)	0	1	7(1)
Si(1)	0	0	2500	1	6(2)
Si(2)	0	2685(4)	2500	1	7(1)
Si(3)	3530(5)	1119(4)	0	1	8(1)

[a] U_{eq} is defined as one third of the trace of the orthogonalized U_{ij} tensor.

Table 3
Bond lengths [Å] for $Eu_2Pt_3Si_5$ at 293(2) K with estimated standard deviations in parentheses.

Label	Distances	Label	Distances
Eu–Si(3) × 1	3.037(2)	Pt(1)–Pt(1) × 9	3.0005(6)
Eu–Pt(2)	3.1465(6)	Pt(1)–Eu × 2	3.4062(5)
Eu–Si(1) × 3	3.1648(5)	Pt(2)–Si(3)	2.410(2)
Eu–Si(2) × 2	3.2265(12)	Pt(2)–Si(2) × 6	2.4381(15)
Pt(1)–Si(3) × 7	2.4790(18)	Pt(2)–Si(1) × 15	2.4507(3)
Pt(1)–Si(2) × 10	2.691(2)	Si(2)–Si(3) × 2	2.534(2)

2.6. Magnetic measurements

Magnetic measurements on bulk samples were performed using single crystalline samples of $Eu_2Pt_3Si_5$ in randomly oriented fashion with a Quantum Design Magnetic Property Measurement System–Superconducting Quantum Interference Device (MPMS–SQUID) dc magnetometer. The purity of all the crystals used in magnetic measurement were checked by single crystal X-ray diffraction using Bruker Smart Apex 2 with a short scans method (total 30 frames with 30 s exposure time). Temperature dependent magnetization data were collected in the field cooled mode (FC) in the temperature range 2–300 K at an applied magnetic field of 1000 Oe. Field dependent magnetization data were collected at 300 and 2 K for $Eu_2Pt_3Si_5$ with field sweeping from -60 to 60 kOe.

2.7. X-ray absorption near-edge spectroscopy (XANES)

X-ray absorption near-edge spectroscopy (XANES) experiments were performed at PETRA III, P06 beamline of DESY, Germany. Measurements at the Eu L$_3$ edge and ambient pressure were performed in transmission mode using gas ionization chambers to monitor the incident and transmitted X-ray intensities. Monochromatic X-rays were obtained using a Si (111) double-crystal monochromator which was calibrated by defining the inflection point (first derivative maxima) of Cu foil as 8980.5 eV. The beam was focused employing a Kirkpatrick–Baez (K–B) mirror optic. A rhodium-coated X-ray mirror was utilized to suppress higher order harmonics. A CCD detector was used to record the transmitted signals. Sample was prepared by mixing an appropriate amount of finely ground powder with cellulose and cold pressing them to a pellet.

3. Results and discussion

3.1. Crystal structure

The crystal structure of $Eu_2Pt_3Si_5$ along c-direction is shown in Fig. 1a. $Eu_2Pt_3Si_5$ crystallizes in the orthorhombic $U_2Co_3Si_5$ structure type with $Ibam$ space group [58]. Akselrud et al. described the $U_2Co_3Si_5$-type structure as an orthorhombic superstructure of the tetragonal $CaAl_2Ga_2$ type [59]. Chabot et al. [60], on the other hand, explained the $U_2Co_3Si_5$ crystal structure as a derivative of two intergrown slabs, one corresponds to $CaBe_2Ge_2$-type structure and the second one belongs to an unknown orthorhombic structure with composition RTM_3 (Fig. 1a). The structure can also be explained as shown in Fig. 1a and b. The two dimensional $[Pt_3Si_5]$ networks (Fig. 1a) are interconnected through the Pt–Si bond along the a-direction resulted an overall three dimensional structure. Eu atoms are removed for the better representation. The $[Pt_3Si_5]$ sheets propagating along bc-plane is shown in Fig. 1b. These puckered sheets are comprised of one dimensional chain of $[Pt_2Si_2]$ and $[PtSi_3]$ tetrahedra propagating along the diagonals of the ab-plane. The puckering develops huge distortion in the sheet, which in fact resulted in eight different types of tetragons in both directions as shown in Fig. 1b.

The shortest Eu–Pt and Eu–Si bond distances in $Eu_2Pt_3Si_5$ are 3.037(2) and 3.1465(6) Å respectively. The Eu–Eu bond distance ranges from 4.1277(6) to 4.2545(6) Å along bc-plane. These bond distances are in line of Eu–Eu bond already reported in the mixed valence compound $EuPd_2Si_2$ (4.1800 Å) [61]. The shortest bond distance can be compared with the Eu–Eu bond distances in other compounds containing only trivalent europium moieties, e.g. Eu–Eu bond distances $EuPd_3$ range from 4.10 to 4.15 Å [62], where as the large distance can be compared with the compounds containing exclusive divalent europium such as Eu_2TGe_3 ($T = Ag$, Au) [1,14] having in the range 4.25–4.35 Å. The non linear arrangement of Eu atoms indicates some sort of disorder in the system. The shortest Pt–Pt, Pt–Si and Si–Si bond distances are 3.0005(6), 2.4790(18) and 2.534(2) Å, respectively. The homoatomic bond distances i.e. Pt–Pt and Si–Si are slightly higher than the sum of the covalent radii reported in the literature (2.74 and 2.34 Å respectively) [63], whereas the heteroatomic bond distance i.e. Pt–Si is close to sum of the covalent radii of Pt and Si (2.54 Å) [63]. The Pt–Si bond distances in this compound are anisotropic in nature, 2.4095(5), 2.6913(24) and 2.4507(3)–2.4794(17) Å along a, b and c directions, respectively. This kind of uneven distribution in bond distances may trigger anomalous behaviors due to modulation to 4f–5d hybridization [1].
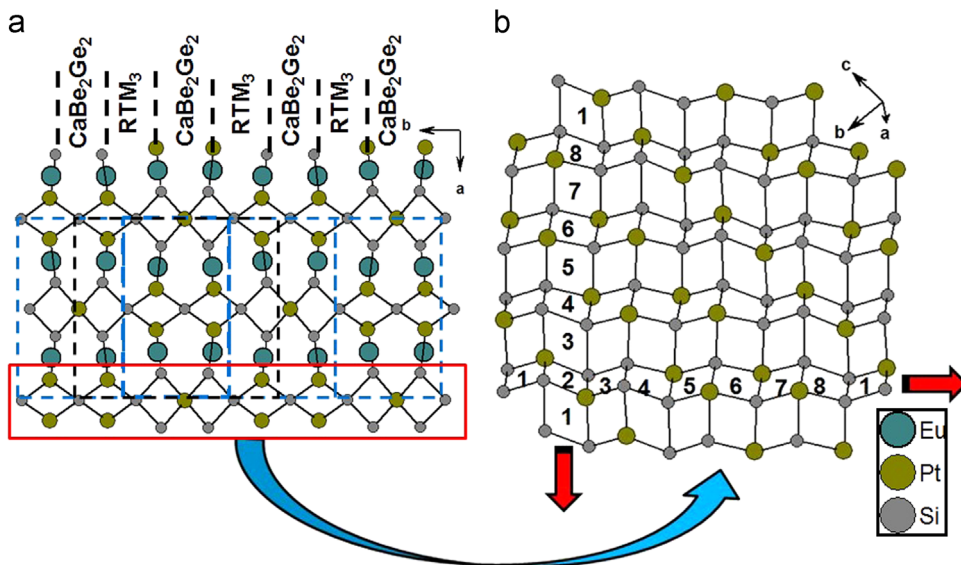
Fig. 1. (a) $Eu_2Pt_3Si_5$ structure as a derivative of $CaBe_2Ge_2$ and RTM_3 type slabs. The units are shown by vertical dashed boxes. Three dimensional network of $[Pt_3Si_5]$ is shown along the *c*-direction, (b) The distorted network of $[Pt_3Si_5]$ consisting of two different one dimensional chains $[Pt_2Si_2]$ and $[PtSi_3]$ propagating along *bc*-plane.

There are six different types of crystallographic sites present in the crystal structure of $Eu_2Pt_3Si_5$; one Eu, two Pt and three Si sites. The coordination environments of all atoms are shown in Fig. S3. Eu resides in a pseudo Frank–Kasper type cage with seven Pt, eight Si and four Eu atoms whereas Pt1 is surrounded by a distorted cuboctahedron environment of $[Pt_2Si_6]$, Si1 and Si2 reside in distorted cuboctahedron geometry of $[Eu_4Pt_4Si_4]$ and $[Eu_4Pt_3Si_5]$, respectively. Pt2 and Si3 reside in trigonal prismatic and tricapped trigonal prismatic environment of $[Si_5]$ and $[Eu_4Pt_3Si_2]$, respectively.

3.2. Magnetic properties

Temperature dependent magnetic susceptibility and inverse susceptibility for the compound $Eu_2Pt_3Si_5$ are shown in Fig. 2. The compound shows two prominent consecutive magnetic ordering at low temperature: the first transition corresponds to antiferromagnetic ordering at 19 K followed by a ferromagnetic transition at 5.5 K. The derivative curve has been shown in the inset, which pinpoints the exact transition temperatures. The inverse susceptibility curve was fitted with Curie–Weiss law in the temperature range of 23–300 K below which it deviated from linearity, the effective magnetic moment/Eu (μ_{eff}) was obtained as 6.78 μ_B/Eu atom and Curie paramagnetic temperature (θ_p), $-$ 45 K. The magnetic moment value is substantially lower than the spin only magnetic moment of Eu^{2+} (7.94 μ_B/Eu atom) hinting toward the presence of mixed valence state of Eu with almost 85% in divalent state, which was later confirmed by XANES studies. The highly negative value of θ_p is indicative of fairly strong antiferromagnetic coupling between the adjacent Eu spins. It further hints toward a possible Kondo behavior in the system [64].

The field dependent magnetic moment at low temperature (2 K) is shown in Fig. 3. At lower magnetic field, the curve adopts a sigmoid shape indicating antiferromagnetic ordering in the compound. The magnetic moment increases with applied field followed by a sudden change in the field higher than 45 kOe. The week hysteresis in higher field is indicative of the sudden spin flop transition from the anti ferromagnetic to metamagnetic state.

3.3. X-ray absorption near edge spectroscopy (XANES)

The substantial deviation of Eu magnetic moment from the spin only value for divalent Eu (7.94 μ_B) led us to believe that it might be in an intermediate or mixed valence state. To unambiguously
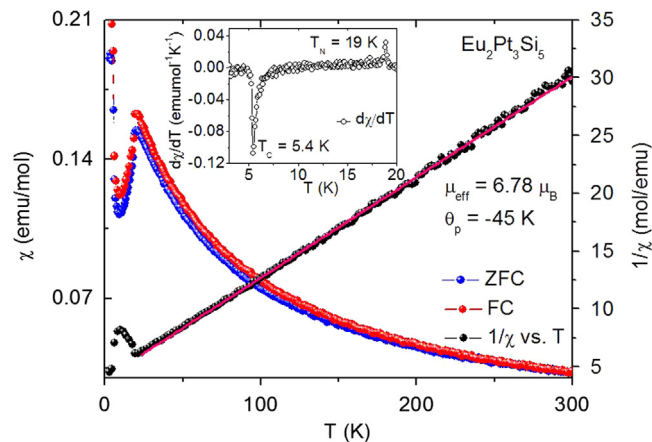

Fig. 2. Temperature dependent molar magnetic and inverse magnetic susceptibility. The inset shows the first order derivative of the magnetic susceptibility.
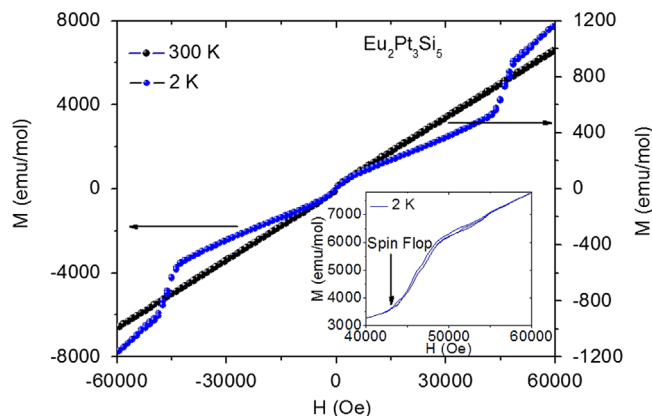

Fig. 3. Field dependent magnetization study on $Eu_2Pt_3Si_5$ sample at 2 and 300 K. The inset shows an enlarged plot of *M* vs. *H* data at 2 K showing spin flop giving rise to metamagnetic transition.

establish the actual valence state of Eu, we have performed XANES, which is a strong experimental tool in order to firmly establish the valence state of an element in a compound. A sharp signal at
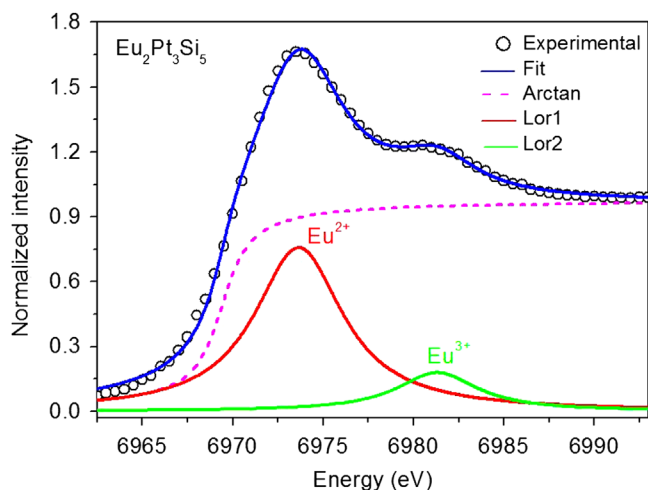
Fig. 4. X-ray absorption near edge spectrum of $Eu_2Pt_3Si_5$ at $Eu–L_3$ absorption edge.

6973 eV was observed in the $Eu–L_3$ X-ray absorption spectrum of $Eu_2Pt_3Si_5$ (Fig. 4). This value is characteristic of the $4f^7$ (Eu^{2+}) configuration and arises due to a $2p_{3/2}$ to $5d$ transition [65]. Another broad hump at around 6984 eV corresponding to Eu^{3+} was also observed [66]. To quantify the ratio of Eu^{3+} to Eu^{2+}, a lorentzian fitting was carried out using 79 data points with 3 line shapes and 9 variables. Integrating over the respective areas yields a ratio of almost 0.18 which means 18% of Eu in this compound is in trivalent state and rest of it i.e. 82% is in divalent state. These results directly corroborate with magnetic susceptibility data, which predicts 85% of divalent Eu in the system.

4. Concluding remarks

Metal flux method has yet gain been successfully used as a strong tool in our continuous search for new intermetallic phases with novel structures and properties. A new rare earth based intermetallic compound $Eu_2Pt_3Si_5$ has been synthesized using indium as an inactive metal flux. The crystal structure was elucidated by X-ray diffraction technique on single crystals. Magnetic measurements revealed mixed valent nature and field induced metamagnetic transition in this compound which is highly interesting in terms of materials points of view. We are currently exploiting similar metal flux strategies to synthesize many other compounds in the $RE_2T_3X_5$ series (RE=rare earth metals, T=transition elements, X=p-block elements) and hope that our work will open up a broader way towards the synthesis and physical property studies of many unexplored compounds.

Appendix A. Supporting information

Supplementary data associated with this article can be found in the online version at http://dx.doi.org/10.1016/j.jssc.2014.12.023.

References

[1] S. Sarkar, S.C. Peter, Inorg. Chem. 52 (2013) 9741–9748.
[2] P. Aynajian, E.H.D. Neto, A. Gyenis, R.E. Baumbach, J.D. Thompson, Z. Fisk, E.D. Bauer, A. Yazdani, Nature 486 (2012) 201–206.
[3] J. Custers, K.A. Lorenzer, M. Muller, A. Prokofiev, A. Sidorenko, H. Winkler A.M. Strydom, Y. Shimura, T. Sakakibara, R. Yu, Q. Si, S. Paschen, Nat. Mater. 11 (2012) 189–194.
[4] J.H. Shim, K. Haule, G. Kotliar, Science 318 (2007) 1615–1617.
[5] L.M. Tran, B. Nowak, V.H. Tran, Phys. Rev. B 84 (2011) 224406–224417.
[6] J.M. Robinson, Phys. Rep. 51 (1979) 1–62.
[7] C.N.R. Rao, D.D. Sarma, P.R. Sarode, E.V. Sampathkumaran, L.C. Gupta, R. Vijayaraghavan, Chem. Phys. Lett. 76 (1980) 413–415.
[8] D.T. Adroja, S.K. Malik, J. Magn. Magn. Mater. 100 (1991) 126–138.
[9] C. Mazumdar, B.D. Padalia, Phys. Rev. B 46 (1992) 9009–9012.
[10] M. Chondroudi, S.C. Peter, C.D. Malliakas, M. Balasubramanian, Q.A. Li, M.G. Kanatzidis, Inorg. Chem. 50 (2011) 1184–1193.
[11] S.C. Peter, M. Chondroudi, C.D. Malliakas, M. Balasubramanian, M.G. Kanatzidis, J. Am. Chem. Soc. 133 (2011) 13840–13843.
[12] C.P. Sebastian, M.G. Kanatzidis, J. Solid State Chem. 183 (2010) 2077–2081.
[13] S.C. Peter, M.G. Kanatzidis, Z. Anorg. Allg. Chem. 638 (2012) 287–293.
[14] C.P. Sebastian, C.D. Malliakas, M. Chondroudi, I. Schellenberg, S. Rayaprol, R.D. Hoffmann, R. Pottgen, M.G. Kanatzidis, Inorg. Chem. 49 (2010) 9574–9580.
[15] U. Subbarao, M.J. Gutmann, S.C. Peter, Inorg. Chem. 52 (2013) 2219–2227.
[16] S.C. Peter, M.G. Kanatzidis, Z. Anorg. Allg. Chem. 638 (2012) 287–293.
[17] S.C. Peter, S. Rayaprol, M.C. Francisco, M.G. Kanatzidis, Eur. J. Inorg. Chem. 2011 (2011) 3963–3968.
[18] C.P. Sebastian, J. Salvador, J.B. Martin, M.G. Kanatzidis, Inorg. Chem. 49 (2010) 10468–10474.
[19] S.C. Peter, S. Sarkar, M.G. Kanatzidis, Inorg. Chem. 51 (2012) 10793–10799.
[20] S.C. Peter, U. Subbarao, S. Rayaprol, J.B. Martin, M. Balasubramanian, C.D. Malliakas, M.G. Kanatzidis, Inorg. Chem. 53 (2014) 6615–6623.
[21] S.C. Peter, U. Subbarao, S. Sarkar, G. Vaitheeswaran, A. Svane, M.G. Kanatzidis, J. Alloy. Compd. 589 (2014) 405–411.
[22] S. Sarkar, M.J. Gutmann, S.C. Peter, Cryst. Growth Des. 13 (2013) 4285–4294.
[23] S. Sarkar, M.J. Gutmann, S.C. Peter, CrystEngComm 15 (2013) 8006–8013.
[24] S. Sarkar, S.C. Peter, J. Chem. Sci. 124 (2012) 1385–1390.
[25] U. Subbarao, S.C. Peter, Inorg. Chem. 51 (2012) 6326–6332.
[26] U. Subbarao, S.C. Peter, Cryst. Growth Des. 13 (2013) 953–959.
[27] U. Subbarao, S. Sarkar, V.K. Gudelli, V. Kanchana, G. Vaitheeswaran, S.C. Peter, Inorg. Chem. 52 (2013) 13631–13638.
[28] U. Subbarao, A. Sebastian, S. Rayaprol, C.S. Yadav, A. Svane, G. Vaitheeswaran, S.C. Peter, Cryst. Growth Des. 13 (2013) 352–359.
[29] Y. Muro, M. Nakano, K. Motoya, J. Phys. Soc. Jpn. 77 (2008).
[30] Y. Muro, M. Nakano, K. Motoya, Phys. B: Condens. Matter 403 (2008) 810–811.
[31] V.K. Anand, Anupam, Z. Hossain, S. Ramakrishnan, A. Thamizhavel, D.T. Adroja, J. Magn. Magn. Mater. 324 (2012) 2483–2487.
[32] S. Noguchi, K. Okuda, Phys. B: Condens. Matter 194–196 (1994) 1975–1976.
[33] C.U. Segre, H.F. Braun, Phys. Lett. A 85 (1981) 372–374.
[34] J. Ge, J. Gutierrez, B. Raes, T. Watanabe, J. Koshio, V.V. Moshchalkov, Physica C 478 (2012) 5–9.
[35] Y. singh, S. Ramakrishnan, Phys. Rev. B 69 (2004) 174423–174436.
[36] N.H. Sung, C.J. Roh, K.S. Kim, B.K. Cho, Phys. Rev. B 86 (2012) 224507–224513.
[37] S. Layek, V.K. Anand, Z. Hossain, J. Magn. Magn. Mater. 321 (2009) 3447–3452.
[38] F. Honda, N. Metoki, T.D. Matsuda, Y. Haga, A. Thamizhavel, Y. Okuda, R. Settai, Y. Onuki, J. Alloy. Compd. 451 (2008) 504–506.
[39] B. Chabot, E. Parthé, J. Less Common Met. 97 (1984) 285–290.
[40] Y. Singh, S. Ramakrishnan, Phys. Rev. B 68 (2003) 054419–054424.
[41] D. Kußmann, R. Pöttgen, G. Kotzyba, J. Solid State Chem. 150 (2000) 112–120.
[42] Y.V. Galadzhun, R.-D. Hoffmann, R. Pöttgen, M. Adam, J. Solid State Chem. 148 (1999) 425–432.
[43] C.J. D., S.G. K., N. D., V.P. J., F.C. M., Phys. Lett. A 79 (1980) 454–456.
[44] Y.P. Yarmolyuk, L.G. Akselrud, E.I. Gladyshevskii, Sov. Phys. Crystallogr 22 (1977) 358–359.
[45] D. Paccard, L. Paccard, J. Less Common Met. 128 (1987) 125–129.
[46] D. Voßwinkel, R. Pöttgen, Z. Naturforsch 68b (2013) 301–305.
[47] M.A. Zhuravleva, M.G. Kanatzidis, Z. Naturforsch 58b (2003) 649–657.
[48] J.M. Kurenbaeva, Y.D. Seropegin, A.V. Gribanov, O.I. Bodak, V.N. Nikiforov J. Alloy. Compd. 285 (1999) 137–142.
[49] V. Mykhalichko, R. Kozak, P. Demchenko, R. Gladyshevskii, in: B. Idzikowski, R. Micnas, P. Leśniak, A. Szajek (Eds.), Proceedings of the European Conference: Physics of Magnetism 2014 Institute of Molecular Physics: Polish Academy of Sciences, Poznań, Poland, 2014, p. 336.
[50] J. Fikáček, J. Prchal, V. Sechovský, Acta Phys. Pol. A 126 (2014) 310–311.
[51] J. Evers, G. Oehlinger, J. Solid State Chem. 62 (1986) 133–137.
[52] I. Mayer, P.D. Yetor, J. Less-Common Met. 55 (1977) 171–176.
[53] D.T. Adroja, B.D. Padalia, S.K. Malik, R. Nagarajan, R. Vijayaraghavan, J. Magn. Magn. Mater. 89 (1990) 375–378.

[54] A. Gribanov, A. Grytsiv, P. Rogl, Y. Seropegin, G. Giester, J. Solid State Chem. 183 (2010) 1278–1289.
[55] SAINT, Bruker AXS Inc., Madison, Wisconsin, USA, 2000.
[56] G.M. Sheldrick, University of Göttingen: Göttingen, Germany, 1997.
[57] G.M. Sheldrick, Structure Determination Program, Siemens Analytical X-ray Instruments Inc., Madison, WI, 1995.
[58] L.G. Akselrud, Y.P. Yarmolyuk, E.I. Gladyshevskii, Sov. Phys. Crystallogr. 22 (1977) 492–493.
[59] L.G. Aksel'rud, Y.P. Yarmolyuk, E.I. Gladyshevskii, Sov. Phys.Crystallogr. 22 (1977) 492–494.
[60] B. Chabot, E. Parthé, J. Less-Common Met. 97 (1984) 285–290.

[61] E.V. Sampathkumaran, L.C. Gupta, R. Vijayaraghavan, K.V. Gopalakrishnan, R.G. Pillay, H.G. Devare, J. Phys. C: Solid State Phys. 14 (1981) L237–L241.
[62] A. Pandey, C. Mazumdar, R. Ranganathan, J. Phys. Condens. Matter 21 (2009) 216002–216006.
[63] J. Donohue, The Structures of the Elements, Wiley, New York, 1974.
[64] G.F. Chen, I. Sakamoto, S. Ohara, T. Takami, H. Ikuta, U. Mizutani, Phys. Rev. B 69 (2004) 054435–054440.
[65] T. Inoue, Y. Kubozono, S. Kashino, Y. Takabayashi, K. Fujitaka, M. Hida, M. Inoue, T. Kanbara, S. Emura, T. Uruga, Chem. Phys. Lett. 316 (2000) 381–386.
[66] K.-B. Kim, Y.I. Kim, H.-G. Chun, T.-Y. Cho, J.-S. Jung, J.G. Kang, Chem. Mater. 14 (2002) 5045–5052.